The Space Technology 8 Mission[1,2]

Stephen Franklin[a], Jentung Ku[c], Brian Spence[b], Mike McEachen[b], Steve White[b], John Samson[d], Rafael Some[a], Jennifer Zsoldos[e]

[a]-Jet Propulsion Laboratory, California Institute of Technology; Pasadena, California
[b]-ATK Space Systems, Goleta, California
[c]-NASA Goddard Spaceflight Center, Greenbelt, Maryland
[d]-Honeywell Defense and Space Electronics Systems, Clearwater, Florida
[e]-Orbital Sciences Corp., Dulles, Virginia

Abstract—The Space Technology 8 (ST8) mission is the latest in NASA's New Millenium Program technology demonstration missions. ST8 includes a spacecraft bus built by industry, flying four new technology payloads in low-Earth orbit. This paper will describe each payload, along with a brief description of the mission and spacecraft. The payloads include a miniature loop heat pipe intended to save mass and power on future small satellites, designed and built by NASA's Goddard Space Flight Center; a lightweight, 35g/m linear mass, 40-m deployable boom intended as a future solar sail mast built by ATK Space Systems; a deployable, lightweight Ultraflex solar array producing 175W/kg, also built by ATK Space Systems; and a high-speed, parallel-processing computer system built of state-of-the-art COTS processors, demonstrating SEU tolerance without the need for radiation-hardened electronics, and 300M operations per second per Watt processing throughput density.

TABLE OF CONTENTS

1. INTRODUCTION 1
2. THERMAL LOOP EXPERIMENT 1
3. SAILMAST EXPERIMENT 4
4. ULTRAFLEX 175 EXPERIMENT 7
5. ADAPTIVE FAULT-TOLERANT COMPUTING (AFTC) EXPERIMENT 9
6. SPACECRAFT DESCRIPTION 12
7. EXPERIMENT OPERATIONS 12
8. SUMMARY 14
REFERENCES 14
BIOGRAPHY 15
ACKNOWLEDGMENTS 15

1. INTRODUCTION

This paper provides an overview of the Spacecraft Technology 8 (ST8) mission. ST8 is run under the NASA New Millenium Program office as well as JPL's Planetary Flight Projects office. ST8 will demonstrate four key technologies, all of which represent substantial improvements over the existing state of these technologies. The first is the Thermal Loop, a small loop heat pipe built and managed by NASA's Goddard Space Flight Center. This experiment will demonstrate mass and power savings, as well as reliable restart capability. The second experiment is a 40m long, extremely lightweight (35g per meter) deployable gossamer boom intended as a future solar sail mast. This is built by ATK Space Systems in Goleta, Ca. ATK Space Systems is also building the Ultraflex 175, a very low mass, 3.2m diameter deployable solar array, intended to demonstrate 175W/kg power density. NASA's Glenn Research Center is also participating in this experiment. Honeywell Corp. in Clearwater, Fl. is building the Adaptable Processor, a triplicate of commercial PowerPC processors which will adapt to measured radiation flux by adjusting the loading across the three processors and working through upsets without shutting down or making a calculation error. This experiment intends to demonstrate 300 million operations per second per watt, a dramatic improvement over state-of-the-art radiation-hardened space flight processors.

ST8 will fly in an elliptical (300km by 1300 km), polar (98.5 degree inclination), sun-synchronous 6 a.m./6 p.m., low-Earth orbit for its 7 month mission. The orbit will take the spacecraft through the van Allen radiation belts each orbit, as well as near both poles, in order to expose the Adaptable Processor to sufficient radiation. The spacecraft will be launched in February 2009 on a Pegasus XL launch vehicle. Orbital Sciences Corporation is also providing the spacecraft bus, experiment integration and test, operations and ground system. The Pegasus launch vehicle is provided by Orbital under contract with Kennedy Space Center's National Launch Services.

2. THERMAL LOOP EXPERIMENT

Overview of the System Design. The Thermal Management System consists of multiple evaporators and multiple condensers, and deployable radiators. Other key elements include thermoelectric coolers (TECs) on the loop heat pipe (LHP) compensation chambers (CCs), a capillary flow regulator, and an aluminum coupling block between the vapor line and liquid line. For the ST8 flight validation, a

[1] 0-7803-9546-8/06/$20.00© 2006 IEEE
[2] IEEEAC paper #1544, Version 2, Nov, 2005

miniature loop heat pipe consisting of two evaporators, two condensers, a body mounted radiator and a deployable radiator will be used, as shown schematically in Figure 1.

The two most important features of the Thermal Loop are the integration of multiple evaporators into a single LHP, and the use of miniature evaporators with an outer diameter (O.D.) of 13mm. As will be elaborated on later, the MLHP combines the functions of variable conductance heat pipes (VCHPs), thermal switches, thermal diodes, and state-of-the-art LHPs into a single integrated thermal system. It retains all the performance characteristics of state-of-the-art LHPs and offers additional advantages to enhance the functionality, performance, versatility, and reliability of the system.

Multiple Miniature Evaporators. An LHP utilizes boiling and condensation of the working fluid to transfer heat, and surface tension forces developed by the evaporator wick to circulate the fluid [1,2]. It can transport large heat loads over long distances with small temperature differences. This process is passive and self-regulating in that the evaporator will draw as much liquid as necessary to be completely converted to vapor according to the applied heat load. When multiple evaporators are placed in parallel in a single loop, each evaporator will still work passively. No control valves are needed to distribute the fluid flows. All evaporators will yield the same vapor temperature as liquid vaporizes inside individual evaporators regardless of their heat loads. The loop provides a single interface temperature for all instruments. Furthermore, when an evaporator is exposed to a heat sink, such as when the attached instrument is turned off, the evaporator will receive heat from other evaporators servicing the operating instruments [3]. This will eliminate the need for supplemental electrical heaters while maintaining all instruments close to the saturation temperature. The evaporators can automatically switch between evaporating and condensing modes based on the surrounding thermal conditions. Therefore, each instrument can operate independently without affecting other instruments.

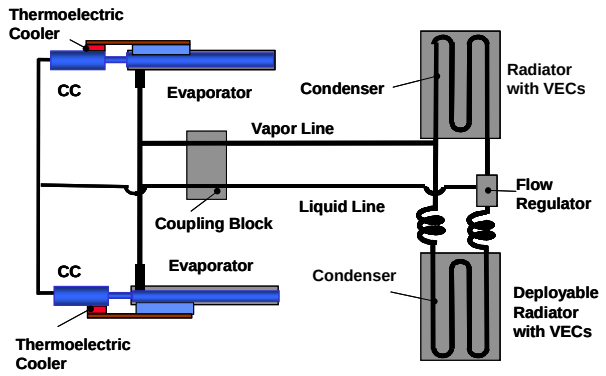

Figure 1 - Schematic of the MLHP Thermal System for ST8 Flight Validation

All evaporators have an outer diameter of 13 mm. The evaporator mass is reduced by 70 percent when compared to 25 mm evaporator used in state-of-the-art LHPs. Small evaporators also reduce the required fluid inventory in the LHP, and the mass and volume of the thermal system.

Multiple Condensers/Deployable Radiators. The fluid flow distribution among multiple, parallel condensers is also passive and self regulating [3, 4]. Each condenser will receive an appropriate mass flow rate so that the conservation laws of mass, momentum and energy are satisfied in the condenser section. If a condenser is fully utilized, such as when the attached radiator is exposed to a warm environment, vapor will be prevented from leaving that condenser by the capillary flow regulator located downstream of the condensers, and any excess vapor flow will be diverted to other condensers. Thus, no heat will be transmitted from a hot radiator back to the instruments, effecting a thermal diode action. Deployable radiators allow both sides of the radiators to dissipate heat, and hence reduce the required radiator area. The radiators can be folded in a stowed position prior to deployment.

TECs: The LHP operating temperature is governed by its CC temperature. The CC temperature as a function of the evaporator power for a given ambient temperature follows the well-known V-shaped curve as shown in Figure 2. The CC temperature can be controlled at a desired set point temperature of T_{set}. The state-of-the-art approach is to cold bias the CC and use electrical heaters to raise the CC temperature. As shown in Figure 2, the CC temperature can be controlled at T_{set} between heat loads of Q_{Low} and Q_{High}. However, this technique does not work for $Q < Q_{Low}$ when cooling of the CC is required.

A TEC attached to the CC can provide heating as well as cooling to control the CC temperature. One side of a TEC can be attached to the CC, while the other side is connected to the evaporator through a flexible copper strap. When the CC is being cooled, the total heat output from the hot side is transmitted to the evaporator and ultimately dissipated to the

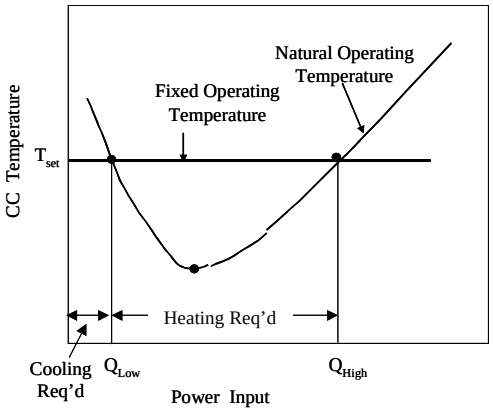

Figure 2 - LHP Operating Temperature

condenser. This is particularly useful during the start-up of the LHP, when a higher heat load to the evaporator is always desirable. When the CC requires heating to maintain its set point temperature in the range of $Q_{Low} < Q < Q_{High}$, the TEC will draw heat from the evaporator. Depending on the efficiency of the TEC, savings on the control heater power can be substantial, especially under the cold sink and high/medium heat load condition.

The operating temperature of the MLHP Thermal Management System can be maintained by controlling any number of CC's at the desired set point temperature [3]. For energy savings, only one CC temperature need be controlled at a time. Control can also be switched from one CC to another at any time. Furthermore, the CC set point temperature can be changed upon command. The ability of the CC to control the loop operating temperature at a constant value makes the MLHP Thermal Management System function as a variable conductance device.

In addition to maintaining the CC temperature, the TECs can be used to enhance the LHP start-up success. A typical LHP start-up involves raising the CC temperature above the evaporator temperature and then applying power to the evaporator. As the evaporator temperature rises above the CC temperature by a certain amount (the superheat), vapor bubbles will be generated in the evaporator and the loop will start, as shown in Figure 3(a). Unfortunately, the required superheat for boiling is stochastic and can range from less than 1 K to more than 10 K. A high superheat can lead to start-up difficulty because, while the evaporator temperature is rising to reach the required superheat, the CC temperature also rises due to the heat leak from the evaporator. Thus, the required superheat for bubble generation may never be attained, as shown in Figure 3(b). This is especially true when a low heat load is applied to the evaporator and a high superheat is required. The net heat load to the evaporator will be small during the start-up transient when the evaporator is attached to an instrument. To overcome the start-up difficulty, the state-of-the-art LHPs use a small-sized starter heater to provide a highly concentrated heat flux to generate first vapor bubbles locally. The required starter heater power is on the order of 30 W to 60 W for standard LHPs with a 25 mm O.D. evaporator. For LHPs with small evaporators, the required starter heater power is estimated to be between 20 W and 40 W.

The TEC attached to the CC can maintain a constant CC temperature, and ensure that the evaporator will eventually overcome the required superheat no matter how high the required superheat and how low the heat load are, i.e. the condition shown in Figure 3(a) will occur. Alternatively, the TEC can be used to lower the CC temperature during the start-up transient to achieve the required superheat as shown in Figure 3(c). Regardless of which method is implemented, the required starter heater power can be reduced or eliminated.

Coupling Block. The coupling block allows the liquid returning to the evaporator/CC to absorb heat from the vapor line, which further reduces the TEC control heater power. Using feedback control, the combination of the TECs and the coupling block can minimize the TEC control heater power.

Analytical Models and Scaling Criteria. An analytical model which simulates the steady state and transient behaviors of LHPs has been developed under a NASA SBIR 2 program [4]. It is used to correlate the MLHP experimental data in laboratory and thermal vacuum tests. Differential equations that govern the operation of LHPs with multiple evaporators and multiple condensers are developed, and a numerical scheme based on the Lagrangian method is employed to solve the equations. This method offers numerical stability and run time efficiency. Most importantly, it yields accurate solutions. The computer code is also very user-friendly.

The LHP operation involves some very complicated fluid and thermal processes, which are strongly influenced by gravitational, inertial, viscous, and capillary forces. To obtain better understanding of fluid flow and heat transfer phenomena in an LHP and to provide a means of comparison and generalization of data between different LHPs, some scaling criteria are needed. Using dimensional

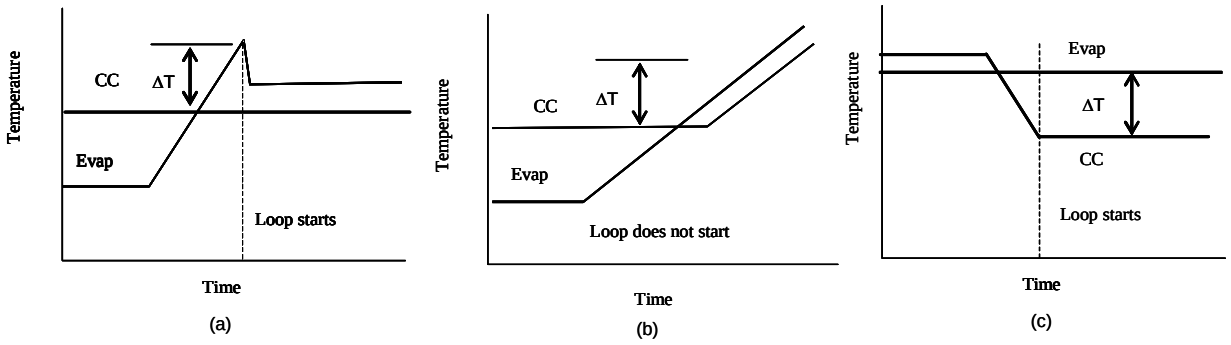

Figure 3 - LHP Start-up

analysis, in combination with known heat pipe phenomena, a set of dimensional and dimensionless groups has been developed to relate geometry and configuration of the LHP components, properties of the wick and the working fluid, and the environmental conditions surrounding the LHP [5].

Technical Advances. Table 1 summarizes the technology advances and advantages of the MLHP Thermal Management System. Most comparisons are made in reference to state-of-the-art single-evaporator LHPs. Major technology advances are: 1) Miniaturization of the evaporator, i.e. reducing the evaporator diameter from 25 mm to 13 mm, 2) Multiple evaporators and multiple condensers in a single LHP, 3) TECs for temperature control and start-up success; and 4) A transient LHP model and scaling rules.

3. SAILMAST EXPERIMENT

Introduction. Gossamer applications pose new challenges in spacecraft architecture consisting in large part of deployable space structure—where mass and stowed volume effectiveness are particularly critical, as these metrics together drive launch costs. Solar sailing [6,7] is the ideal

example: very large structures are required, and low mass is crucial since thrust is inversely proportional to the mass needed to deploy and stabilize the reflective sails. The volume of the stowed sail system must not drive the payload to a larger launch vehicle, as this may offset the cost savings of this new propulsion technology. Stiffness is not generally a driving requirement, since it has been accepted by the gossamer community that the sailcraft attitude and trajectory control system must be engineered to function with the gossamer structure's modal response is critical to the viability of these structures in real applications [8]. Therefore, a gossamer truss has slender, strength-driven structural elements. As elements are made more slender, they become more susceptible to waviness. This waviness is caused by the manufacture of the composite and by minute inaccuracies in assembly from bay to bay. Additionally, since the truss itself is slender it is also subject to global bow and twist from manufacturing inaccuracy and thermal distortion. In the gossamer regime the potential range of local and global imperfections can combine in complex ways to reduce load-carrying capability.

The work described herein was performed under a Concept Definition (study phase) contract. The experiment under development for the ST8 flight program is a Scalable Architecture for the Investigation of the Load Managing Attributes of a Slender Truss. The SAILMAST experiment plan provides a thorough investigation of the fundamental attributes of an ultra-lightweight (slender) coilable truss, allowing extrapolation to generalized gossamer truss structures that may be different in geometry, loading, or design (Figure 4). These efforts will reduce the risk to the first users of gossamer structure technologies, allowing incorporation into science missions to occur at an accelerated pace. The SAILMAST experiment will provide validation of the most fundamental building block of gossamer space structure technology and, in particular, the essential element needed for near term solar sailcraft to support key NASA roadmap missions.

For the ST8 Concept Definition Phase, a 7-m length of gossamer SAILMAST structure was built and tested in a 1 g (laboratory) environment. This technology stows in less than 1% of its deployed length. The linear mass of this structure is 34 g/m, which is less than 15% of the mass of comparable flight heritage structures and less than 50% of the mass of the sail mast structure built in 2003 under the NASA In-Space Propulsion (ISP) Solar Sail Ground System Demonstrator program [9,10]. Static and dynamic bending tests of this most advanced gossamer structure were performed and correlated with a Finite Element Model

Table 1 - Technology Advances of MLHP Thermal Management System.

Technology Item	State-of-the-Art	MLHP Technology Advances
Integral Thermal Subsystem – MLHP with TECs on CCs	Louvers, Heat Pipes, LHPs, Heaters, Thermostats	Flexible Locations of Heat Dissipating Components, Heat Load Sharing, TEC for Temperature Control and Start-up Enhancement
LHP Configuration	Single Evaporator	Multiple Evaporators
LHP Evaporator Diameter	25 mm O.D.	13 mm O.D.
Analytical Modeling of LHPs	Top-level Transient Models for Single Evaporator LHPs. No Scaling Rules	Detailed Transient Models for Multi-Evaporator LHPs Scaling Rules Established
LHP Start-up Method	Starter Heaters on Evaporator (20W to 40 W)	TEC on CC (<5W)
LHP Temperature Control	Control Heater on CC; Cold Biased, Heating Only, No Cooling Heater Power: 5 W to 10 W	TEC on CC plus Coupling Blocks on Transport Lines; Both Heating and Cooling Heater Power: 0.5 W to 2 W

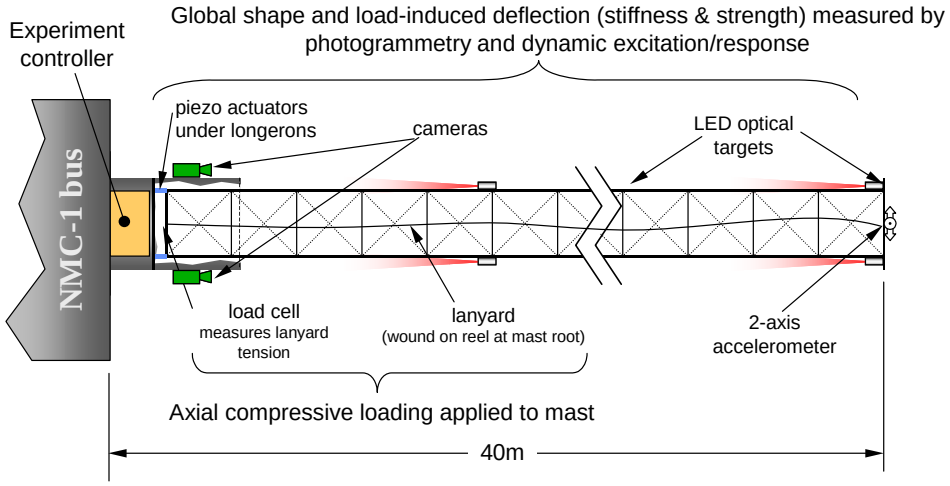

Figure 4 – SAILMAST

(FEM) of the test system as well as a newly developed analytical treatment for slender trusses. This effort has brought the technology readiness level (TRL) to 4. The follow-on activities in the Formulation Refinement and Implementation phases are planned to increase the experiment definition with progressively higher-fidelity analysis tools, hardware, and test environments.

Technology Validation Experiment Objectives. In order for the flight experiment to be considered a success it must measure the global shape of the mast and obtain the degree of bow, and it also must quantify the load capability of the mast. Measured results must have sufficient fidelity to allow identification of the influence of separate effects, i.e. photogrammetric measurement of global bow must be sufficiently accurate to discern distortions that have an effect on strength within the predictive accuracy of the analysis. By looking at sources of error, and correlation with hardware testing performed during the Study Phase, a reasonable assessment of our analytical predictive accuracy has been achieved. The model correlates with test results within 3%, in the range tested so far. Further insight into the performance of long slender booms will be possible with refinements to the model made after testing and correlation with the full-length test boom, as well as a reduction in predictive error. The scalability of the experiment's results will be established by dual-measurement-method correlation of test results with predicted values. The two data acquisition methods are independent and are configured to capture similar data with a similar level of accuracy.

Parametric studies will be performed on the 40-m boom in order to access validity of the model under a wide range of potential circumstances. In particular, the global bow can be deliberately adjusted by external means, and the stiffness and load capability assessed. This will enable flight data acquisition throughout a range of possible free-state shape conditions. Along with validating the applicability range of the analytical model, the hardware itself will prove out the range of possible global distortion that may be accommodated by the loading and imaging techniques planned for flight.

The performance of the flight structure will, of course, be investigated in the laboratory environment prior to flight. The SAILMAST will be supported to negate, to the extent

possible, the effects of gravity on shape. Load versus deflection experiments, analogous to the flight regimen, will be measured and compared with those predicted by the models, accounting for measured global and local shape. In order to provide a range of data points for analytical correlation, known distortions will be induced to the local and global mast shape. Mast displacement will be measured both by the flight video method and by a laser target tracker. While true free-state shape will be impossible to generate in 1g, measuring the shape in two orthogonal positions, then combining the data will approximate the 3-d shape. This data can then be input to the FEM and the analytical model, and sources of variance diagnosed. By the end of this phase, there will be high confidence in the precision of predictive capability provided by the analytical model.

The planned Formulation Refinement activity includes fabrication of the flight experiment mast, while the Implementation Phase will provide the remainder of the flight hardware involved in the experiment. This will allow system-level testing to be performed, ensuring that the experiment will function as planned and provide the desired measurements, with the range and precision required to achieve the post-flight TRL of 7. The 40-m structure will be integrated with the stowage canister, hold-down release and other structure and mechanisms used for flight, as well as video, telemetry and accelerometers necessary for the in-flight experiment. The complete system will be tested as proto-flight hardware to establish final mass properties, functional deployment capability, stowed sine and random vibration testing, thermal cycling survivability, and deployed stiffness and buckling strength.

Validation Flight Experiment Scenario. The in-space experiment will begin by deploying the SAILMAST from the stowage canister, to zenith, by paying out a lanyard with a motor. Upon full deployment, a baseline measurement of mast shape will be performed by photogrammetric analysis of targets as imaged by a video camera mounted at the mast root. Actuation of piezos in line with the longerons at their root will induce small oscillations of the structure as a sine input is swept. The tip accelerometer and videogrammetry will observe the first mode response amplification, and the damping after the input force succession. The mast shape will then be entered into the mast sizing spreadsheet. Next, the motor will be slowly reversed, pulling on the lanyard, until a known axial load has been applied to the boom, as measured by a load cell on the lanyard pulley. This load will have produced some displacement in the mast, to be measured by again taking images with the root camera. This process is repeated at several loads until additional lanyard stroke does not increase lanyard load, at which point the mast will be “buckled”. The load is then reduced, and images taken as before, at increments until the load has been fully removed.

Predictive Models. The analytical models developed during the Concept Definition phase are covered in depth in reference [11], and are summarized below. A detailed finite element model of the mast was assembled, incorporating details such as initial longeron waviness, unique end conditions (from the actuators). The model was run using large-deflection (nonlinear) analysis tools, and generated predicted load/deflection curves for various initial waviness and bow conditions. The FE results were compared against predictions made by closed-form models coupled with an iteratively solving computer spreadsheet. This combination of models (FE and closed-form) provided a powerful set of tools for predicting peak axial load based on initial conditions, and leaves only the task of validating the models with real mast hardware. A significant amount of correlation will be achievable within the confines of the Earth (gravity) environment, including length scaling and sensitivity to initial conditions by external adjustment of mast shape.

In-Flight Experiment Operation. In conjunction with the boom technology, there are a number of unique elements required to execute the SAILMAST flight experiment, particularly related to the challenge of operating the experiment remotely. Remote testing requires the use of specialized actuators and sensors that must operate effectively in the particular regime applicable to our experiment. The standard methods used for ground-based structural characterization are not practical in flight, and the realities of the flight experiment environment must be accounted for in the analytical modeling.

The planned in-flight test configuration has been designed to accommodate a wide range of initial global bow and capture the maximum load capability. The deflection at maximum load for all foreseeable initial conditions falls within the limits of measurable deflection.

Videogrammetry. The deployed free-state shape of the gossamer structure has a significant effect on its axial load carrying capability, and this relation is a fundamental investigation of the SAILMAST experiment. A simple yet robust method for measuring this shape is provided by photogrammetry. Targets placed at discrete stations along the length of the (zenith-pointed) mast are visible as distinctly bright spots in an otherwise dark image, and the location of those spots will be analyzed to determine the shape of the boom.

The SAILMAST experiment will utilize a version of a flight-proven video system. The video system consists of a camera, lens, and controller unit. The requirements for this system are driven by the conditions of the proposed experiment, and relate to the capability of resolving distortions in the boom that affect its stiffness. A spreadsheet has been developed to calculate these requirements, based on camera pixel density, optical clarity, depth of field, and target distance. As may be seen in Figure 5, all the targets are still visible from the root, and

therefore may be used to indicate the relative straightness of the boom.

The common assumption for photo-based measurements is that a super-high resolution image is required to provide sufficient accuracy for meaningful data. This results in very high hardware development cost, as well as burdensome data rates. The SAILMAST experiment benefits from the fact that the targets to be tracked are close together, so the field of view of the imager can focus on a narrow field of view. This optimizes the amount of data captured by the available pixels, and means that a standard space flight imaging sensor will provide sufficient definition to resolve boom distortions of the magnitude significant to strength performance. For example, the standard video-imaging sensor with a 75 mm focal length lens, on a 40-m boom can potentially resolve as little as 2.2 mm of tip displacement, which translates to a 2% uncertainty on load capacity. Assessing these requirements has indicated that the imaging specifications are neither too stringent, resulting in high

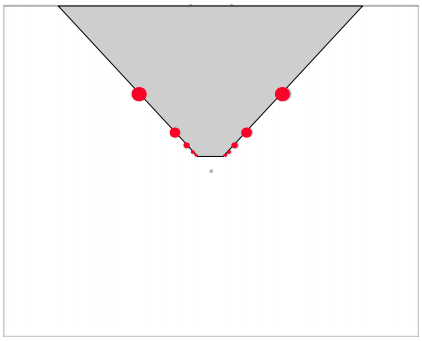

Figure 5 - Simulated view down mast

development cost and risk, nor too relaxed to provide adequate measurement of global shape.

Once the video data files are downloaded, the mast deflection and dynamics are interpreted using optical target tracking software. This software calculates X- and Y- target positions frame by frame, with the Z- axis (along the mast length) positions pre-programmed, and used to scale the motion of the targets. This data will be compared with predicted performance and any discrepancies will be diagnosed.

4. ULTRAFLEX 175 EXPERIMENT

The Ultraflex 175 is designed and built by ATK Space Systems, in collaboration with the NASA Glenn Research Center (GRC) and EMCORE Photovoltaics (EPV). This solar array is an innovative technology advance that provides leapfrog performance over the state-of-the-art. NGU is an accordion fanfold flexible-blanket solar array comprised of ten primary interconnected isosceles-triangular shaped ultra-lightweight substrates. The major NGU subsystem assemblies and their nomenclature, depicted in the stowed and deployed states, are shown in Figure 6. When deploying in a rotational “fan” fashion, each interconnected triangular shaped substrate (also known as a gore) unfolds; upon full deployment the structure becomes tensioned into a rigid shallow umbrella-shaped structure. Radial spar elements attached to each substrate elastically deflect to predetermined positions when completely deployed to maintain the deployed structure in a preload and high-stiffness state.

Current state-of-the-art solar arrays systems are based on rigid composite honeycomb panel construction. These existing systems are heavy, provide low deployed first mode natural frequencies, and occupy a large stowage volume. The NGU system achieves break-through performance through an innovative technology advance composed of a flexible-blanket accordion-folded lightweight membrane that is deployed to a tensioned and rigid pre-loaded structure (similar to a shallow umbrella structure).

The triangular gores are the building blocks of the NGU system, consisting of an open mesh Vectran substrate to which the cell circuits are bonded using a patented ultra-lightweight process. The use of the lightweight open mesh substrate allows the NGU to have a very low non-power producing mass per unit area, and allows the cells to radiate directly from their (partially open) backsides. When stowed, the NGU array gore substrates are folded in a flat-pack accordion manner and sandwiched between two rigid panels (static and pivot panels) to produce a compact launch volume. The static and pivot panels serve as rigid platens reacting the internal cell/foam stack preload in the stowed configuration. Thin open-cell polyimide foam strips, discretely attached to the substrate backside, act as protective interleaves between each blanket fold and provide robust protection (and high damping) for the delicate PV from severe vibration environments. The entire stowed package is preloaded between the static and pivot panels by the launch restraint/release system (tie-downs).

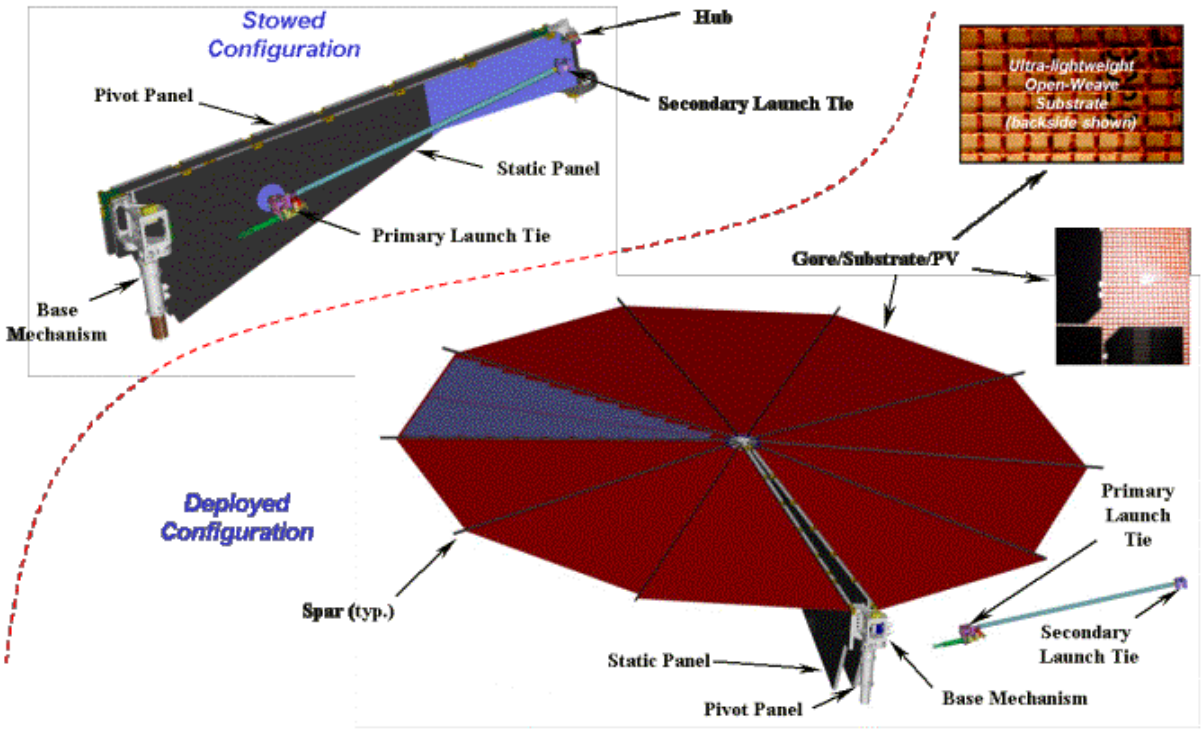

Figure 6 - Major Ultraflex 175 Subsystems and Assemblies

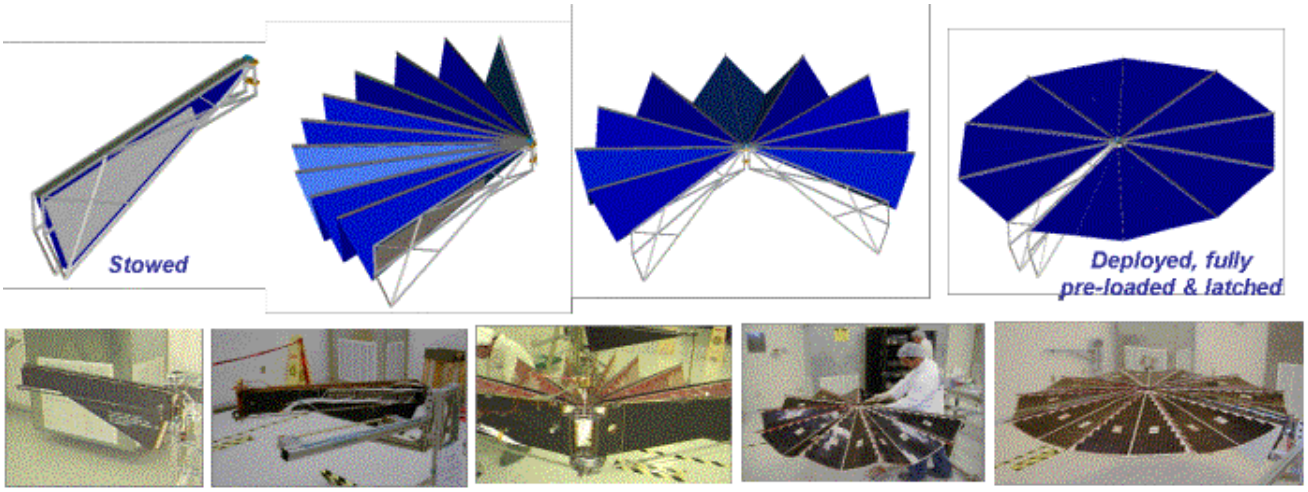

Figure 7 - Ultraflex 175 Deployment Sequence

Deployment is initiated by tie-down release. The NGU deployment sequence is a two-staged process and is shown in Figure 7. Upon tie-down release, the stowed package becomes loosely contained and begins a rotational articulation away from the spacecraft about the base mechanism to a final staging location where its position is latched and secured (staging shown is 90 degrees, but can be any angle). Once initial staging is complete, the final deployment stage is initiated through a proven motor-driven lanyard assembly. The lanyard, attached to the pivot panel, is continuously reeled onto the motor pulley; hence rotating the pivot panel and unfurling the NGU blanket nearly 360 degrees to its final deployed state. Upon final deployment, the NGU spars deflect and the blanket simultaneously tensions to produce a deployed shallow-umbrella (paraboloid) shaped structure that is a preloaded membrane having exceptionally high deployed-stiffness for its size.

The NGU solar array combines structural performance and the highest available specific power with a very low stowed volume and footprint. NGU achieves its deployed strength and stiffness from lightweight radial spar members that allow tensioning of a flexible blanket populated with solar cells. This unique structural system allows the use of a flexible blanket without requiring massive secondary structure (such as a heavy mechanical or inflatable boom) to

deploy and tension the wing as is common in other flexible substrate solar array systems.

The NGU is a highly evolved version of ABLE's 1st generation UltraFlex design [12], developed for flight under ABLE IR&D and the NASA Mars 01-Lander program (MSP 01) for Lockheed Martin Space Systems Company and the Jet Propulsion Laboratory. In support of the MSP 01 program ABLE developed, built, and flight qualified two 1st generation UltraFlex flight wing systems. Each wing was populated with SHARP 17% efficient silicon PV and the entire array system (i.e., two wings) supplied almost 900 watts BOL. The (relatively small) system was designed to deploy in a 1g environment with no external off-loader. The resulting specific power of this 1st-generation UltraFlex technology for the Mars 01-Lander was 103 W/kg BOL (a factor of two increase over the NMP DS1 SCARLET concentrator array) [13,14]. Pictures of the UltraFlex Mars 01-Lander wing are shown in Figure 6.

The proposed NGU baseline system offers exceptional scaled-up performance exceeding the NMP ST8 requirements, and provides many additional features desired by NASA. In addition, many breakthrough technologies are proposed to be developed/implemented within the NGU system to provide significant performance growth capability. Descriptions of these new features and their rationale for implementation are provided in Table 2. The systematic maturation and implementation of these advanced subsystem technologies will result in numerous NGU solar array system benefits, each with the potential to optimize or enable a particular spacecraft mission application. The proposed NGU technology enhancement and resulting performance growth will demonstrate the potential and flexibility of the NGU to be the standard high-performance solar array platform for future NASA, commercial and military space missions.

5. ADAPTIVE FAULT-TOLERANT COMPUTING (AFTC) EXPERIMENT

The AFTC will validate a computing architecture, coupled with methods of fault tolerance which, together, will allow the use of advanced commercial-parts-based high performance computing in moderate space-radiation environments.

Many next generation space missions will require onboard high performance processing for science, as well as on-board data analysis. Current space-qualified computing

Table 2 - NGU Performance versus ST8 Requirements and NASA Needs

Parameter Description	ST8 Requirement and/or NASA Need	NGU Predicted Performance for a 7-kW sized wing system	Comments/Justification
BOL specific power	>175 W/kg for a 7-kW wing system	>175 W/kg for NGU-S >220 W/Kg for NGU-LW	ST8 requirement met with standard MJ PV. Much higher specific power achievable with lightweight MJ PV. The NGU platform provides "road map" growth beyond the ST8 requirement
Deployed first mode frequency	> 0.1 Hz	> 0.3 Hz	Extremely lightweight tensioned structural platform with sufficient depth provides deployed stiffness significantly higher than classical systems
Stowed specific volume	> 31.8 kW/m^3	> 33 kW/m^3	NGU occupies an extremely compact launch volume and footprint compared to classical systems
High voltage capability	> 100 VDC operation	> 100 VDC operation	NGU is inherently suited to high voltage operation because of its serpentine circuit configuration/layout and lack of conductive substrate. Conventional high voltage design solutions can be applied to NGU at lower mass than classical systems.
Multi-A.U. Operation capability	to 5 A.U.	to 5 A.U.	NGU employs use of EPV ATJ PV. These devices have undergone preliminary LILT testing and shown their suitability for multi-A.U. missions. NGU high-temp capability materials also allow for < 1.0 operation.
Scalability	7 kW wing size	to 15 kW wing size and beyond	The NGU is scalable to wing sizes beyond 7 kW with the simple optimization of spar structural elements (to optimize bending and torsional stiffness). Recent studies for advanced JPL applications have sized NGU wings as high as 12 kW.

Parameter Description	ST8 Requirement and/or NASA Need	NGU Predicted Performance for a 7-kW sized wing system	Comments/Justification
Stowed transfer orbit power	N/S	Provides stowed transfer orbit power	NGU provides the ability to incorporate stowed transfer orbit power (need for most GEO-comsat missions), enhancing commercialization (addressed in Study Phase)
Radiation hardness	Operation in high radiation environment	Operates in high radiation environments	NGU employs proven radiation hard MJ PV technologies. Rear side and front side shielding can be applied to increase radiation hardness.
Reliability	High reliability	High reliability	NGU is a high-reliability system because of its simple and redundant mechanisms and features, and its 1st generation heritage from the UltraFlex Mars 01-Lander system
Cost	Low (Reasonable)	Low (Reasonable)	NGU has the ability to be cost-competitive with classical systems once completely developed and its significant mass benefits are included in overall mission costs. The simplicity of the mechanical design and low cost substrates should allow for NGU recurring costs to be no greater than classical systems.

systems, built around radiation hardened processors, can not provide sufficient performance, e.g., throughput, or throughput per watt, to meet these requirements. In terrestrial laboratories, science data processing is performed on parallel processing cluster computers. Similarly, the complex models envisioned for future highly autonomous robotic systems also need high performance, parallel or supercomputer architectures to meet near real-time requirements. A cluster computer comprises a set of single board computers, interconnected by a high-speed switched network, running a file-oriented multi-threading operating system and a "middleware" which controls and coordinates parallel processing applications. A typical system might consist of 10 to 20 Motorola G4 based single board computers, interconnected via a gigabit Ethernet, running the LINUX operating system and an MPI middleware. The parallel processing applications are typically written in a version of FORTRAN, C or C++ and are supported by parallel math libraries such as ScaLAPACK or PLAPACK. In the most advanced architectures, Field Programmable

Gate Arrays (FPGAs) are used to implement the algorithms directly in hardware. FPGAs allow configuring of hardware "on the fly", and provide the most power and time efficient implementations of mathematical routines.

Over the past few generations, Commercial off the Shelf (COTS) computer components have become much more resistant to the debilitating effects of radiation. Many commercial parts can withstand many 10s of kilorads of Total Ionizing Dose (TID) and are immune to catastrophic Single Event Latchup (SEL). The primary issue preventing the deployment of a spaceborne cluster computer is their continued susceptibility to Single Event Upsets or SEU's, (aka soft errors). Uunlike TID and SEL, SEUs only cause a bit flip from 1 to 0 or 0 to 1, and do not cause permanent damage. Further, in the latest generation of computer electronics, Silicon On Insulator (SOI) CMOS, has proven to be approximately an order of magnitude less susceptible to SEU than previous bulk CMOS. If we can withstand a few errors per day per processor, without unduly impacting system dependability, it would be possible to fly, essentially commercial, cluster computers. Not only would this provide mission enabling performance, but it would significantly lower the cost of development as standard laboratory science codes could be easily ported to these systems without the expensive and error prone process normally associated with moving complex codes from the lab to a new platform.

The Honeywell AFTC experiment will validate the technological concept, the architecture, the fault tolerance techniques and the associated performance, reliability and availability models behind this technology. Supplementing ground-based testing, the in-space validation will test those aspects of the technology which can not be effectively exercised on the ground. This includes the ability to withstand concurrent omni-directional, multi-species, multi-energy, and extremely high energy radiation while meeting required reliability and availability levels. The experiment will also provide the data required to calibrate the associated models and to allow scaling of the models to radiation and computing environments well beyond the ST8 LEO/MEO environments.

Figure 8 shows the AFTC hardware architecture. It consists of a radiation hardened Power PC (PPC) 603e based single board computer which acts as a controller for a parallel

processing cluster of COTS based PPC750 compute nodes. Interconnection of the parallel processing cluster is via Gigabit Ethernet. An additional memory card simulates a global mass store. The software stack in Figure 9 shows the software architecture, including the middleware layers which provide fault tolerance for the cluster. The middleware layer also includes a thin isolation layer which makes porting between platforms a minimal and straightforward process.

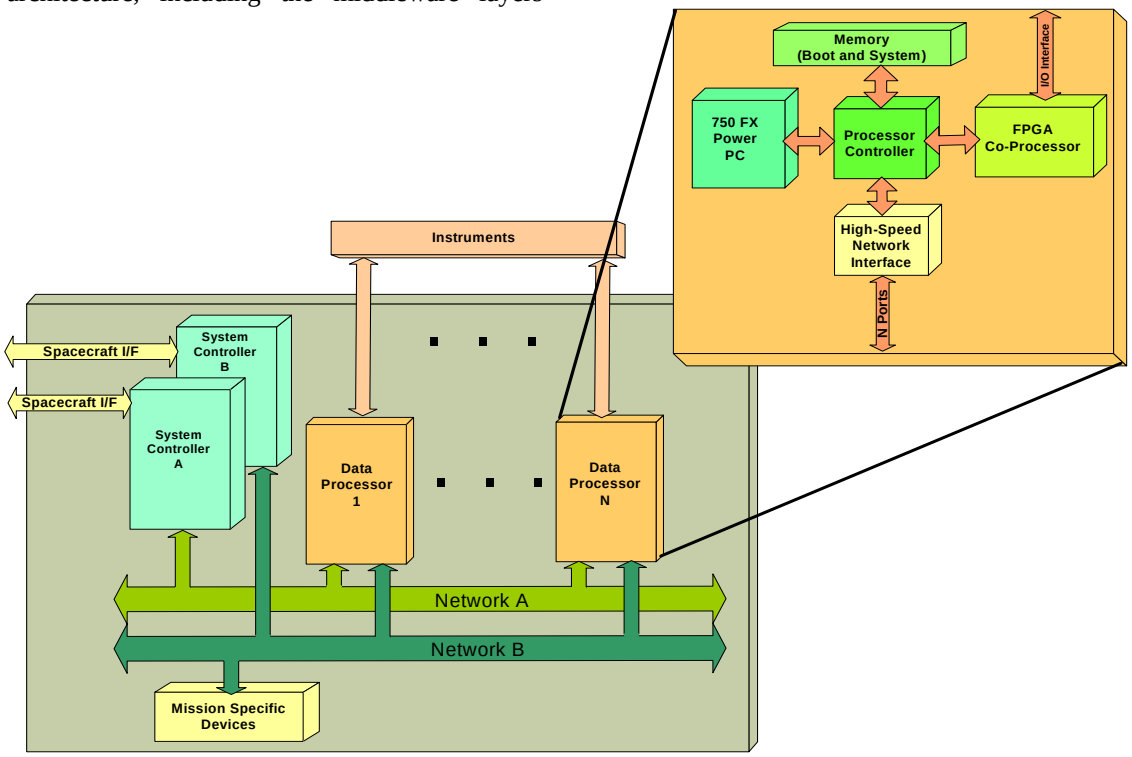

Figure 8 - Hardware Architecture.

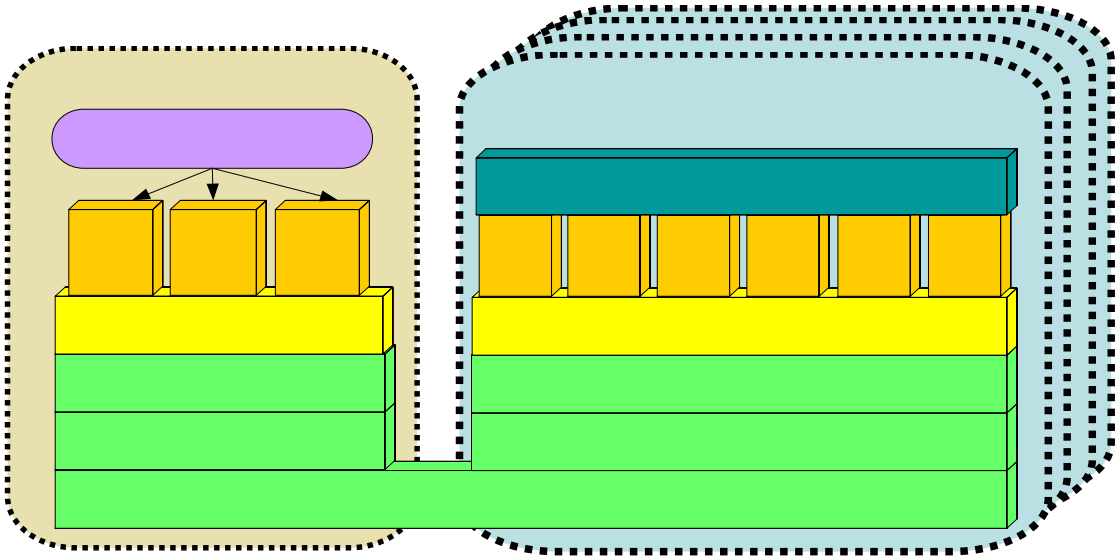

Figure 9 - Software Architecture

The objectives of the AFTC experiment are four-fold: 1) to expose a COTS-based, high performance processing cluster to the real space radiation environment; 2) to characterize the radiation environment; 3) to correlate the radiation performance of the COTS components with the environment; and 4) to assess the radiation performance of the COTS components and the AFTC system response in order to validate the predictive Reliability, Availability, and Performance models for AFTC and for future NASA missions.

The AFTC flight experiment will encompass measurement of component and system parameters that can only be validated in a real space environment. Primarily, these are the component fault/error rates dues to radiation, and the accuracy of the predictive fault/error model. These data will support the experiment objectives identified in the previous paragraph. The spacecraft ephemeris will be used to correlate the radiation performance of the COTS components with the orbit location. Other technology validation data, including cluster performance, cluster performance per watt, error detection and recovery latencies, Operating System overhead, and Fault Tolerant Middleware overhead, will be collected in ground-based technology validation experiments. These parameters do not need to be re-validated in space because they are not expected to change from the values measured during the ground-based experiments.

Except for some power-up and initialization testing, whenever the AFTC payload is powered, AFTC operation is expected to be a free running experiment, collecting radiation environment characterization and radiation event (SEU) data, correlating the environment and detected events with S/C orbit location, and monitoring and reporting AFTC response. The AFTC experiment is expected to be run continuously for four of the six month ST-8 mission to maximize the amount of data collected.

6. SPACECRAFT DESCRIPTION

The Orbital Sciences spacecraft bus combines two product lines from Orbital's small low-Earth orbit spacecraft: a LEOStar-2 structure and MicroStar avionics. 39 MicroStar spacecraft have been launched to date and 8 more are in production or have been delivered for launch. The

ORBCOMM constellation, NASA's QuikTOMS satellite, and the FORMOSAT-3 satellites are all MicroStar vehicles; Orbview-4 and NASA's GALEX, SORCE, AIM, and OCO spacecraft are LEOStar-2 vehicles.

The spacecraft, pictured in Figure 10, consists of a small 14-inch high hexagonal aluminum honeycomb bus, a vertical payload module mounted on top, and 4 deployable solar array panels attached to the hexagonal bus. The bus structure contains all the spacecraft bus components, including electronics, battery, sensors, and actuators. The aluminum honeycomb payload module holds all 4 experiments and associated electronics. It provides cooling to the Adaptive Processor experiment and thermal isolation to the other three experiments. The spacecraft mass is limited by a Pegasus lift to orbit of 250 kg (current estimate is approximately 160 kg) and produces approximately 558 watts in sunlight (at a 32 degree sun angle).

Attitude Control. The spacecraft will be maintained in a nadir-pointing attitude throughout the mission, with the SAILMAST pointing at zenith and the Ultraflex 175 on the anti-velocity side of the spacecraft. A single Y-axis reaction wheel provides a momentum bias and pitch control. Magnetic torquers are used for roll/yaw control and to dump reaction wheel momentum. The pointing requirements are very loose: 5 degrees in control and knowledge and 2 degrees knowledge of angle from Ultraflex to sun vector. Neither gyro nor star tracker is required, so the sensors are limited to coarse and fine sun sensors, Earth sensors, and a magnetometer.

An on-board GPS receiver is used for spacecraft position and time knowledge.

Power. The spacecraft is powered by four GALEX-heritage deployable solar panels, which provide approximately 558 watts at a 32 degree sun angle. Eclipse operation is to be supported by a Li-Ion battery; however, a Li-Ion versus NiH_2 battery trade is currently being performed.

Command & Data Subsystem. The command and data handling architecture is comprised of a set of three distributed processors; these are the flight computer, the battery control regulator, and the attitude and control electronics. A mission interface unit will provide RS422 data interfaces to each experiment and will provide data storage. Uplink and downlink communication is provided by an S-band Transceiver and dual omni antennas.

7. EXPERIMENT OPERATIONS

Mission operations is conducted out of Orbital's Mission Operations Center on their Dulles, Va. campus. The experimenters will be present to monitor critical operations, such as deployment of the SAILMAST and Ultraflex 175 solar array. During normal operations, data will be sent from Orbital to the experimenters' facilities via the internet (see Figure 11). JPL will coordinate multiple activity requests among the experimenters in order to derive an

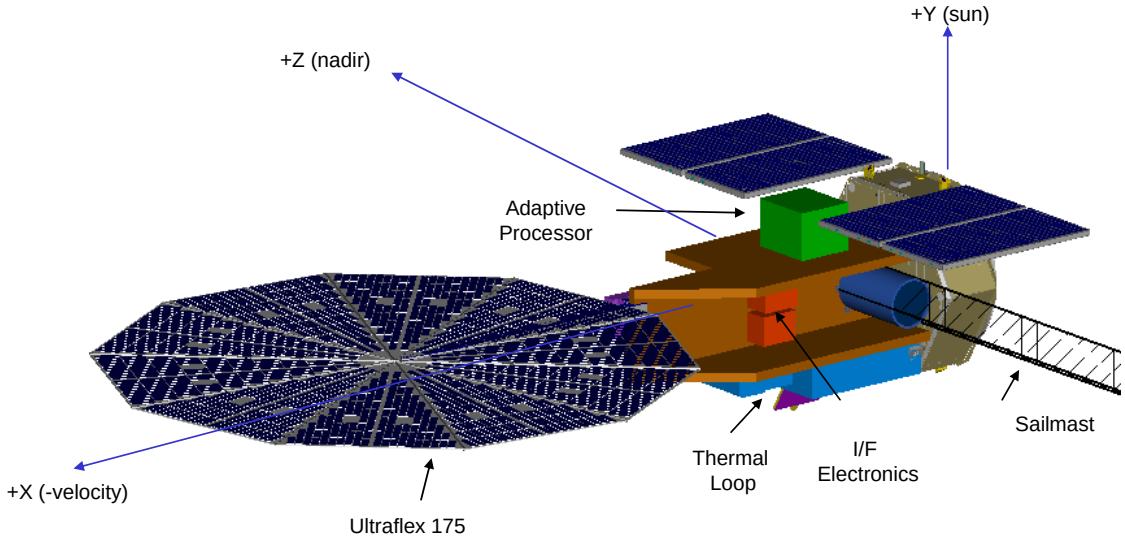

Figure 10 - ST8 Spacecraft

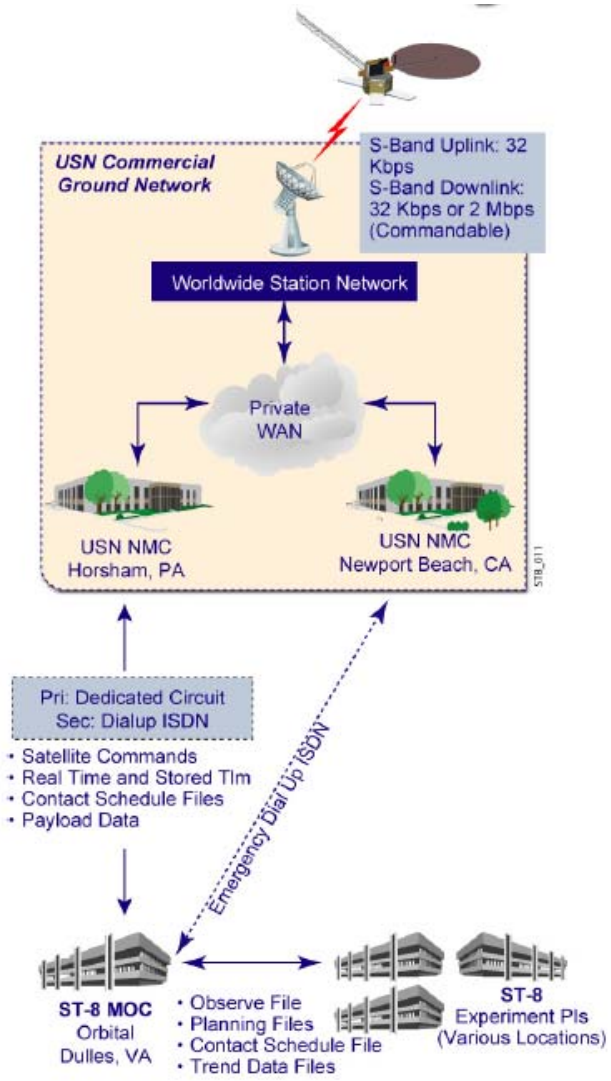

Figure 11 - Operations Locations

activity plan. Experimenters will forward command sequences to JPL and Orbital, at which point the sequences will be reviewed and then uplinked to the spacecraft.

The current operations scenario calls for performing the Ultraflex 175 deployment and experiment operations as the first experiment activity following a one month spacecraft checkout. This activity will only take a few days, at most. The Thermal Loop and AFTC experiments will both be performed over a longer term, perhaps for much of the 6 month experiment operations phase, in order to collect data during several of the experiments' modes. The final experiment activity will be the SAILMAST deployment and subsequent structural tests. This experiment is performed last in order to reduce the risk of a failure impacting the spacecraft or other experiments.

8. SUMMARY

NASA's ST8 mission will demonstrate four major technology advances that will each enable future planetary and Earth-orbiting missions.

REFERENCES

[1] Maidanik, Y. F., et al., "Heat Transfer Apparatus," United States Patent No. 4515209.

[2] Ku, J., "Operating Characteristics of Loop Heat Pipes," SAE Paper No. 1999-01-2007, 1999.

[3] Ku, J, and G. Birur, "Testing of a Loop Heat Pipe with Two Evaporators and Two Condensers," SAE Paper No. 2001-01-2190, 2001.

[4] Hoang, T, O'Connell, T., and J. Ku, "Mathematical Modeling of Loop Heat Pipe with Multiple Evaporators and Multiple Condensers, part I: Steady State Simulation," AIAA Paper No. AIAA-2004-0577, 2004.

[5] Mishkins, D., et al., "Non-Dimensional Analysis and Scaling Issues in Loop Heat Pipes," 41st AIAA Aerospace Science Meeting and Exhibit, Reno, Nevada, January 6-9, 2003.

[6] Mclnnes, C. R., Solar Sailing: Technology, Dynamics and Mission Applications, 1st ed, Springer-Praxis. London, 1999.

[7] Murphy, D., Murphey, T., and Gierow, P., "Scalable Solar-Sail Subsystem Design Concept," AIAA Journal of Spacecraft and Rockets, Vol. 40, No. 4, pp. 539-547, July-August 2003.

[8] Murphy, D., and Wie, B., "Robust Thrust Control Authority for a Scalable Sailcraft," 14th AAS/AIAA Space Flight Mechanics Meeting, AIAA, Washington DC, 2004.

[9] Murphy, D., Trautt, T., McEachen, M., Messner, D., Laue, G., and Gierow, P., "Progress and Plans for System Demonstration of a Scalable Square Solar Sail," AAS 04-105, 14th AAS/AIAA Space Flight Mechanics Meeting, AIAA, Washington DC, 2004.

[10] Murphy, D., Macy, B., and Gaspar, J., "Demonstration of a 10-m Solar Sail System," 45th AIAA Structures, Structural Dynamics, & Materials Conference, 5th Gossamer Spacecraft Forum, Palm Springs, CA, April 19-22, 2004.

[11] McEachen, M., Trautt, T., and Murphy, D., "The SAILMAST Flight Validation Experiment", AIAA-2005-1884, 46th AIAA Structures, Structural Dynamics, & Materials Conference, 6th Gossamer Spacecraft Forum, Austin, TX, April 18-21, 2005

[12] "A High Specific Power Solar Array for Low to Mid Power Spacecraft," P. Jones, Steve White, Jeff Harvey, & Brian Smith, 1994 SPRAT

[13] "The SCARLET Array for High Power GEO Satellites (B. Spence, Dave Murphy, P. Alan Jones, and Michael I. Eskenazi), 26th IEEE Photovoltaic Specialists Conference, September 1997

[14] "The EOS-AM Solar Array" R. Kimber & O. Regalado, 1993 IEEE Conference

BIOGRAPHY

Steve Franklin *is the flight system manager on ST8. Previously, he was the flight system manager on MTO during its study phase, and the Mission Assurance Manager during formulation development, until the mission was cancelled. Before that, he led the autonomy development on Boeing's Spaceway mission; delivered avionics hardware for the X33 Launch vehicle for AlliedSignal; and designed the fault protection algorithms for the Mars Pathfinder spacecraft at JPL. Steve has a B.A. in physics and math from the University of Colorado, a master's degree in electrical engineering from the University of Southern California, and an M.B.A. in finance from the Anderson School at U.C.L.A. sfrankli@jpl.nasa.gov. 818-393-3384.*

Jentung Ku *bio*

Brian R. Spence*, Senior Program Manager - Brian R. Spence received his B.S.M.E. from the University of California, Santa Barbara, in 1986 and has over 16 years experience in space deployable solar array and structural systems. Mr. Spence has been involved in the management, design, development, analysis, production and test of deployable structures, mechanisms, and solar array systems (rigid panel, flexible blanket, thin film blanket, and concentrator technologies) in project engineering and program management capacities. The most relevant programs/technologies to this paper include: PI for the current ST8 Next Generation UltraFlex Study Phase, Mars Dust Mitigation Development Program (under subcontract to JPL), NASA Advanced Thin Film UltraFlex, CellSaver concentrator, PowerSail/SquareRigger, HS702 AstroEdge concentrator, and the NASA SSTI AstroEdge concentrator solar array systems. Mr. Spence is a technical staff member of the ABLE solar array systems group, has authored numerous technical papers, has three awarded patents, has received a NASA Achievement Award, and is a registered professional engineer in the state of California.*

Steve White*, Technical Director - Steve White received his Bachelors and Masters of Science in Mechanical Engineering, with honors, from the University of California, Santa Barbara, in 1983 and 1986, respectively. Mr. White has worked solely on space deployable structures and solar array systems for the past 13 years. Mr. White has been involved in the design, development, analysis, production and test of deployable structures, mechanisms, and solar array systems in project engineering, technical director and management capacities. The most relevant programs to this paper include: Co-I for the current ST8 Next Generation UltraFlex Study Phase, the Mars Dust Mitigation Development Program (under subcontract to JPL), Mars 01 Surveyor Program Lander UltraFlex Solar Array, the GPS IIF solar array, the PUMA BSAT-2C PUMA solar array, and the PUMA INDOSTAR solar array system. Mr. White is a co-author of numerous technical papers, and has received two NASA Achievement Awards.*

Mike McEachen *bio*

John Samson *bio*

Rafael Some *bio*

Jennifer Zsoldos *is the spacecraft lead system engineer on ST8. Ms. Zsoldos earned a B.S. in Aerospace Engineering from Virginia Polytechnic Instutute, and a M.S. in Engineering Management from University of Maryland. She has been workiing in the spacecraft field for over 14 years. Ms. Zsoldos began working in GSFC's Flight Dynamics Facility at CSC as an engineer performing orbit and attitude dermination for NASA missions, and has been working at Orbital Sciences Corporation for the last 10 years in Attitude Determination and Control and Systems Engineering. Her recent responsibilities have included GALEX ACS Lead Engineer, ACS Analysis & Simulation Department Manager, and Systems Engineering New Business Capture Lead for ST8.*

.

ACKNOWLEDGMENTS

This research was carried out in part at the Jet Propulsion Laboratory, California Institute of Technology, under a contract with the National Aeronautics and Space Administration (NASA). Parts of this work were also performed at the NASA Goddard Spaceflight Center and the NASA Glenn Research Center.

Reference herein to any specific commercial product, process, or service by trade name, trademark, manufacturer, or otherwise, does not constitute or imply its endorsement by the United States Government or the Jet Propulsion Laboratory, California Institute of Technology.

The work in Section 2 was sponsored by NASA Goddard Space Flight Center under TBD Contract TBD. The opinions, interpretations, conclusions, and recommendations are those of the author and not necessarily endorsed by the United States Government.